Environ. Sci. Technol. **2008,** *42,* 5235–5240

An Empirical Approach to Estimating Detection Limits Using Collocated Data

NICOLE P. HYSLOP* AND WARREN H. WHITE

Crocker Nuclear Laboratory, One Shields Avenue, University of California, Davis, California 95616

Received October 4, 2007. Revised manuscript received March 31, 2008. Accepted April 23, 2008.

Measurements of trace species generally become less certain as concentrations decrease. Data analysts need guidance on the ranges in which particular measurements are meaningful. This guidance is normally stated in the form of detection limits. The International Union for Pure and Applied Chemistry (IUPAC) has defined several parameters to characterize measurement detection limits (Currie, L. A. *Pure Appl. Chem.* 1995, *67*, 1699). The published guidelines envision an ability to prepare reference materials with concentrations close to the detection limits using the same methods as for normal samples. For multianalyte methods such as X-ray fluorescence (XRF), multiple reference materials may be required for each analyte to characterize the effects of interferences. The creation and characterization of such complex reference materials at the detection limits of modern XRF systems represents a considerable technical challenge. This paper describes an observational approach to estimating the detection limits defined by IUPAC. Our empirical approach takes advantage of collocated (duplicate) measurements that are routinely collected by the Interagency Monitoring of Protected Visual Environments (IMPROVE) network and Speciation Trends Network (STN). The analysis is successfully demonstrated by deriving detection limits at the measurement system level for six elements measured on $PM_{2.5}$ samples by XRF in both networks. The two networks' detection limits are found to be similar in terms of loading (areal density, ng cm^{-2}) on the filters as measured by the XRF instruments despite many differences in sample collection, handling, and analysis. IMPROVE detection limits are an order of magnitude lower than STN's in terms of atmospheric concentrations (ng m^{-3}), because IMPROVE uses smaller filters and higher flow rates which lead to more concentrated sample deposits.

Introduction

Detection capabilities are fundamental performance characteristics of a measurement process. They must be characterized in order to identify marginal data and to design a measurement process that meets specified goals. This paper takes advantage of existing quality assurance data to develop an empirical approach to estimate detection limits.

Properly defined detection limits address two subtly different questions (*1*). The first question often arises after the measurement is made: At what threshold of reported concentrations can we be confident that the analyte is truly present? The second question arises when evaluating a measurement program: At what minimum actual concentration can we be confident that the analyte will be measured? These questions are familiar in forensic and clinical settings where two types of errors are distinguished: false positives, often called type I errors, and false negatives or type II errors. Our confidence in detection limits is expressed in terms of the rates at which we expect to make these errors. Measurement distributions are required to characterize these error rates.

Figure 1 illustrates both types of detection errors with actual measurement distributions from the IMPROVE program. The histograms on the left in both graphs depict the distribution of measured loadings from 374 network field blanks. The histograms on the right depict the distribution of replicate XRF analyses of two lightly loaded sample filters. False positives arise from the variation of blank Si; a few blanks have loadings that are well above the mean loading of the real sample. False negatives arise from the variation measured on V sample loading, which went undetected (zero loadings) in several XRF analyses even though the mean reported loading (1.7 ng cm^{-2}) was seven times the reported minimum detection limit (MDL).

Detection limits are inherently resource-intensive to characterize because they are based on knowledge about the behavior at the outside edges of the distributions. Large amounts of data are required to characterize the edges of a distribution relative to characterizing the central tendencies of the distribution. For example, the United States Environmental Protection Agency's (USEPA) guidance for wastewater analyses requires a confidence level of 99% in the detection limit (*2*). If 100 randomly selected blanks are analyzed to establish this level, the probability is 0.99^{100} (>36%) that none of the measurements will be in the top percentile of the overall blank population. Therefore, unless the exact form of the distribution is known *a priori*, hundreds of analyses are required to characterize the 99% confidence level.

The concept of detection has been complicated over the years by inconsistent and incomplete definitions (*3–5*). Several rigorous approaches have been proposed for estimating meaningful detection limits (*2, 3, 6–10*), all relying on the availability of standard reference materials of specified compositions at arbitrarily low concentrations. These are difficult to implement for routine multielement analyses of environmental samples, where testing would have to cover a wide range of potential interferences and matrix effects. XRF analyses instead customarily report a lower limit of detection based on some multiple of the statistical uncertainty in the background counting rate (*11*). This addresses the hypothetical question of the least concentration that can be measured under ideal conditions in the absence of any interfering species. Both STN and IMPROVE report variants of this limit with their data, the STN value being identified as the "method detection limit" (*12*) and the IMPROVE value as the "minimum detectable limit" (*13*). Following the networks' practices, the common acronym MDL will be used in this paper for both parameters.

IUPAC Detection Limit Definitions. In 1995, the International Union of Pure and Applied Chemistry (IUPAC) published recommendations for "Nomenclature in evaluation of analytical methods including detection and quantification capabilities" (*1*). The publication includes definitions of detection limits to avoid type I and type II errors.

* Corresponding author fax: (530) 754-8979; e-mail: Hyslop@crocker.ucdavis.edu.

10.1021/es7025196 CCC: $40.75
Published on Web 06/19/2008

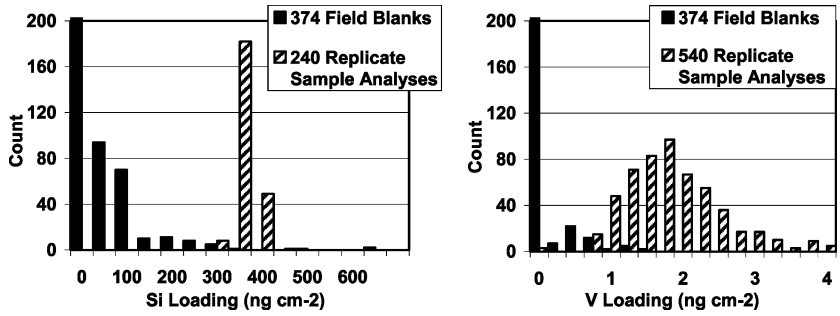

FIGURE 1. Measurement histograms of 374 field blank filter analyses and multiple analyses of a single lightly loaded sample filter for Si (left) and a different lightly loaded sample filter for V (right).

It will facilitate the discussion of the IUPAC recommendations to first introduce some terminology and notation. The value sought by a measurement will be identified with L, the mean outcome expected from many repetitions of the measurement. This convention allows for our usual ignorance of a measurand's "true" value. An individual measurement will be denoted by $\hat{L}$. The probability that A is true given that B is true will be written Pr(A|B).

To avoid type I errors a *critical limit* L_c is set such that measurements above that limit indicate the analyte is present with a high level of confidence. For a given probability α of type I error, L_c is the minimum value satisfying the inequality

$$\Pr(\hat{L} > L_c | L = 0) \leq \alpha \quad (1)$$

An error rate of $\alpha = 5\%$ is commonly considered tolerable and will be adopted here. Measurements above L_c provide confidence that the analyte is present above background, but the converse is not true; measurements below L_c do not quantify confidence that there is no analyte present. Practical examples of type I error are mistaking sample contamination or analytical noise for positive concentrations. Figure 2 shows an idealized example of blank filter variations (i.e., measured $\hat{L}$ when $L = 0$) and the location of L_c relative to that distribution. The type I error rate is represented by the area labeled "α"; in this area, the blank measurements are greater than L_c and indicate that the analyte is present (false positive). The blank distribution in Figure 2 is illustrated by a dashed line to the left of the mean because the blank mean is often zero and values below zero may not be reported; this fact must be considered if the blank distribution is modeled by a normal distribution.

To avoid type II errors, a *limit of detection* L_D is set such that atmospheric concentrations of the analyte at or above that threshold will be detected with a high level of confidence. L_D is dependent on L_c because the analyte must be measured above L_c to be considered present. For a given probability β of type II error, L_D is the minimum value satisfying the inequality

$$\Pr(\hat{L} < L_c | L = L_D) \leq \beta \quad (2)$$

A rate of $\beta = 5\%$ for type II error will be accepted in subsequent analyses. L_D can be substantially higher than L_c when other components of a sample interfere with the measurement of the target analyte. Figure 2 illustrates an ideal measurement distribution with a mean concentration of exactly L_D. The type II error rate is represented by the area labeled "β"; in this area, the measured concentrations are less than L_c and are interpreted as indicating that the analyte is not present (false negative). Note that the α and β areas are adjacent because the depicted sample mean is exactly L_D.

Materials and Methods

Data from IMPROVE and STN are used in this analysis. Both networks use a variety of analytical techniques to measure

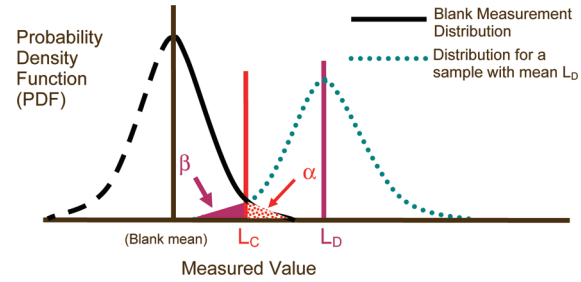

FIGURE 2. Illustration of the detection limit definitions using idealized measurement distributions of blank filters and a sample with a mean value of L_D where L_c is the critical value, α is the type I error rate, L_D is the limit of detection, and β is the type II error rate (*1*).

elements, ions, and carbonaceous species in airborne particulate matter with aerodynamic diameters less than 2.5 μm ($PM_{2.5}$). This paper focuses on determining the detection limits for six elements measured by XRF analysis: Ti, Mn, Cu, As, Se, and Pb. The following subsections briefly summarize the operations and XRF measurements in these two air quality monitoring networks.

Sampling Techniques. IMPROVE is designed to characterize current visibility and aerosol conditions in scenic areas (primarily national parks and forests). The IMPROVE network collects $PM_{2.5}$ samples on filter media over 24-h periods every three days at approximately 170 sites across the United States (US). IMPROVE sites are primarily located in rural or remote locations. The samplers used in IMPROVE were designed by the University of California in Davis (UCD). The samplers use a flow rate of 22.8 lpm and collect XRF samples on 25 mm diameter Pall Corporation Teflo™ PTFE membranes with a sample deposit area of 3.53 cm^2. More information about the network can be found on the project Web site, http://vista.cira.colostate.edu/improve/.

STN is designed to support the National Ambient Air Quality Standards (NAAQS) for $PM_{2.5}$ and provides data on the chemical composition of $PM_{2.5}$. STN collects $PM_{2.5}$ samples over 24-h periods every three or six days at 54 sites across the US. STN sites are primarily located in urban and suburban areas. Three different types of samplers are certified for use in STN: MetOne SASS, Andersen RAAS, and URG MASS. The vast majority of the sites use SASS samplers. This analysis only uses samples collected with SASS samplers to limit the number of variables. The SASS samplers use a flow rate of 6.7 lpm and collect XRF samples on 47 mm diameter Whatman PTFE Teflon membranes with a sample deposit area of 11.3 cm^2. More information about STN can be obtained at http://www.epa.gov/ttn/amtic/specgen.html.

XRF Measurements. Energy-dispersive XRF analysis (EDXRF) is used to analyze both the IMPROVE and STN samples. EDXRF is a nonselective analytical technique, meaning that it does not focus on each element individually. Instead, a range of X-rays is directed at the sample filter, and

all elements present in the sample with absorption bands in that range are excited and measured simultaneously. The advantage of EDXRF systems is that they provide rapid multielement results. XRF analysis is based on the principle that atoms emit X-ray photons of characteristic energies when excited by an external energy source. A silicon−lithium detector is used to count the photons and determine their energies (*11*).

The XRF instruments and peak identification software used to analyze the IMPROVE samples were designed and constructed by UCD. Twenty-four elements between Na and Pb are reported from the XRF analyses. Two separate XRF systems, one with a copper anode (Cu-XRF) for the lower atomic number elements (Na through Fe) and another with a molybdenum anode (Mo-XRF) for the higher atomic number elements (Ni through Pb), are employed to measure the elements. A major change to the UCD Cu-XRF instrument was made in the middle of the data set used for this analysis, replacing a He purge of the analysis chamber with a vacuum environment (*14*). This change provides a cleaner spectral background and improves sensitivities for the lightest elements (*15*). The energy spectra from both systems are reduced to elemental loadings by a custom software program (*16*) that integrates peak counts and applies the relevant calibration factors. If no local peak is discernible in an element's assigned energy range, a nondetect (zero loading) is reported.

STN reports concentrations of 48 elements, including the 24 elements reported by IMPROVE. Research Triangle Institute (*17*) performs the majority of the XRF analyses for STN using two ThemoNoran QuanX instruments, and Chester Laboratories analyzes a fraction of the filters using two Kevex instruments (models Delta 770 and 771). All these instruments analyze the samples in a vacuum environment. Instead of using different anodes, these instruments use a single rhodium (Rh) anode X-ray tube along with several filters to obtain different source X-ray energies to preferentially excite subgroups of elements.

Blank Filters. IMPROVE collects field blanks at random sites at a rate of approximately 1% of the routine samples. IMPROVE field blanks are loaded into cassettes, transported to the site, loaded into the sampler, left in the sampler for a week along with the sample filters, and transported back to the laboratory just like routine samples. The only difference is that ambient air is never pulled through the field blank filters. All XRF data from blank filters collected during 2004 through June 2006 were included in this analysis. This amounted to a total of 454 blank filters analyzed by the Cu-XRF instruments and 568 blank filters analyzed by the Mo-XRF instrument. IMPROVE does not publicly report blank filter data. The blank data used in this analysis were obtained directly from UCD.

STN reports data from field and trip blanks, respectively collected at rates of 10% and 3% of the routine samples (*18*). The STN field blanks are loaded into the sampler and then immediately removed and returned to their containers; they are not left in the sampler with the sample filters as the IMPROVE field blanks are. Trip and field blank data for 2004 through 2006 were used in this analysis and were downloaded from http://www.epa.gov/ttn/airs/airsaqs/detaildata/downloadaqsdata.htm on January 25, 2007.

Collocated Sampling. IMPROVE began installing collocated samplers in October 2003, and the installations continued through December 2004 (*19*). There are seven duplicate samplers spread throughout the network. Data through May 2006 were used in this analysis. Most of the IMPROVE collocated data used in this analysis were downloaded from the VIEWS Web site (http://vista.cira.colostate.edu/views/) on 29 June 2007. The Phoenix collocated data are not available from VIEWS and were obtained directly from UCD.

STN started operating collocated samplers in 2000 (*20*). SASS samplers are used at five of the six collocated sites. Data from 2003 through 2006 were used in this analysis. The STN collocated data were extracted from AQS (http://www.epa.gov/ttn/airs/airsaqs/detaildata/downloadaqsdata.htm/) in May 2007.

Analysis and Discussion

The XRF instruments measure sample loadings (or densities) in units of elemental mass per filter collection area (ng cm^{-2}). The analyses that follow present the XRF measurements directly in these terms. A final summary graph then reinterprets the results in terms of concentrations in air, accounting for the differing sample volumes and filter sizes employed by IMPROVE and STN.

Of the 24 elements measured by both IMPROVE and STN, six are included in this analysis: Ti, Mn, Cu, As, Se, and Pb. These six elements were chosen with both objective and subjective criteria. Most importantly, the element had to be measured at a wide enough range of concentrations to span its L_D at the collocated sites in both networks. Fourteen of the twenty four elements met this criterion; the remaining ten elements were either always above or below their L_D. Of the fourteen elements with adequate ranges, a few showed unusual behaviors. The lightest atomic weight elements were affected by the change from a He purge to vacuum in the IMPROVE Cu-XRF and were excluded for that reason. Of the remaining elements, six were selected to provide representative examples.

Critical Limit, L_c, Estimates. L_c, as defined by IUPAC, is the minimum significant measured value. L_c is dependent on the sample collection and preparation techniques, the sample media, the sensitivity of the instrument, and analytical interferences. The combined effect of these factors, excluding analytical interferences, can be estimated by analyzing blank filters. To avoid making assumptions about the distribution, L_c is set equal to the 95th percentile blank measurement, providing a type I error rate of $\alpha = 5\%$.

L_c's are estimated for the entire period in each network from XRF analyses of the field blanks for IMPROVE and of the trip and field blanks for STN. The STN trip and field blanks were combined because RTI reports that the distributions have shown little difference (*18*). Figure 3 shows the Ti, Mn, Cu, As, Se, and Pb loadings for the IMPROVE and STN blanks collected and analyzed from 2004 through 2006. The *y*-axis shows the percentile corresponding to the blank filter loading on the *x*-axis. Most elements are not detected (i.e., loading is reported as zero) on the majority of blank filters; the percent of nondetects for an element is indicated by the percent at which the curve begins. For example, Ti was not detected on 52% of the STN blank filters and was not detected on 58% of the IMPROVE blank filters. In all six graphs, the STN blank measurements begin at lower loadings than the IMPROVE measurements. This pattern persisted for all 24 of the XRF elements reported by both networks and is likely related to differences in the spectral processing software.

Table 1 summarizes the L_c estimates. The agreement between the L_c's in the two networks is interesting given that the filters are from different manufacturers and are treated differently in the two networks. Despite the fact that the IMPROVE blanks are exposed to the ambient environment for longer periods of time, they do not show consistently higher loadings than the STN blanks. These L_c's will be used to estimate L_D's.

Limit of Detection, L_D, Estimates. L_D is the minimum concentration at which the analyte is reliably detected and measured as significant. This requires $1-\beta$ probability that the measured value will be above L_c. Interfering elements can

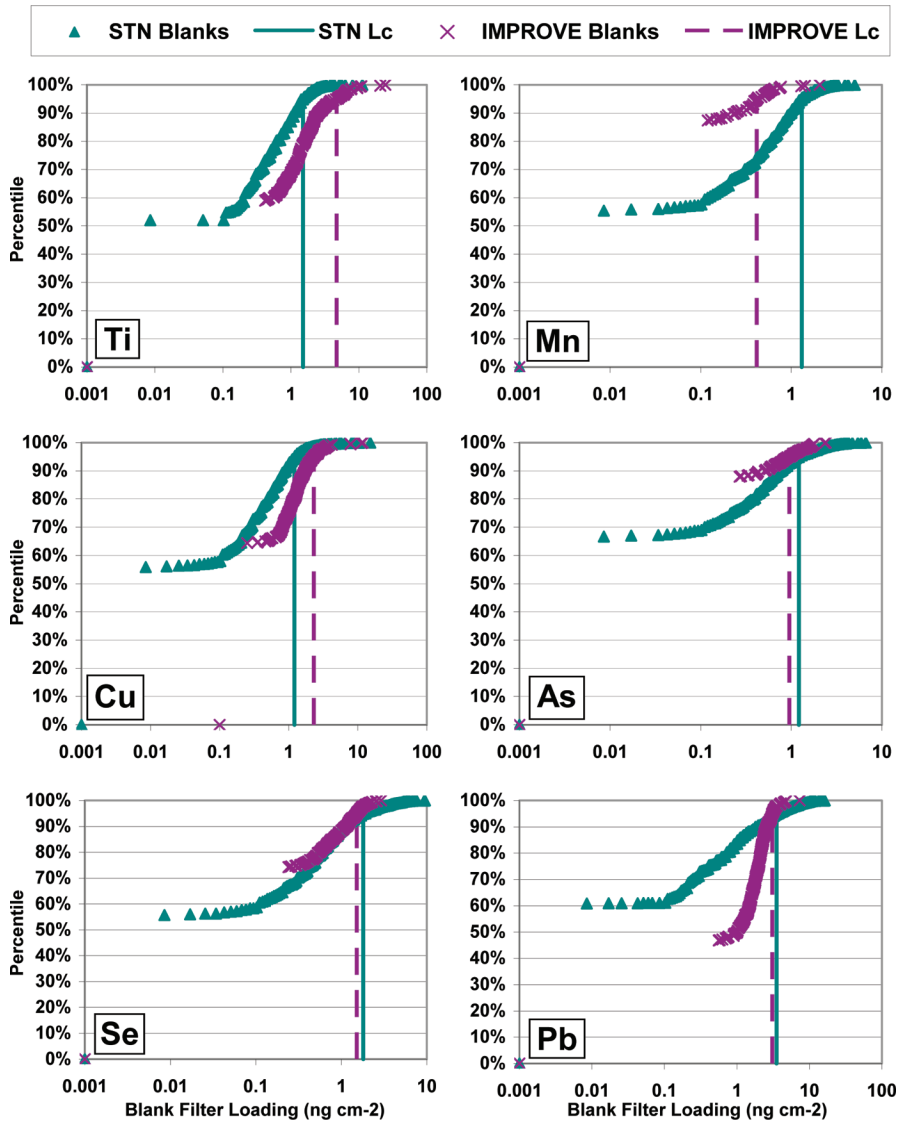

FIGURE 3. STN and IMPROVE blank filter distributions for (a) Ti, (b) Mn, (c) Cu, (d) As, (e) Se, and (f) Pb.

TABLE 1. Summary of STN and IMPROVE L_c estimates, L_D estimates, and MDLs Reported by the Respective Network

element	network	L_c 95th percentile (90−99th percentiles) (ng cm^{-2})	L_D 95% detection probability (92−97% probability) (ng cm^{-2})	reported MDL mean ± standard deviation (ng cm^{-2})
Ti	STN	1.5 (1.1−2.4)	6.0 (5.2−11)	3.7 ± 2.3
	IMPROVE	4.7 (2.6−9.5)	8.0 (7.2−100)	0.32 ± 0.05
Mn	STN	1.3 (1.0−2.2)	3.8 (3.0−4.7)	1.9 ± 0.6
	IMPROVE	0.41 (0.24−0.75)	3.0 (1.6−10)	0.29 ± 0.06
Cu	STN	1.2 (0.9−2.5)	3.4 (2.8−5.1)	1.8 ± 0.3
	IMPROVE	2.3 (1.7−3.7)	3.6 (3.4−3.9)	0.6 ± 0.2
As	STN	1.2 (0.7−2.6)	3.7 (3.4−7)	1.9 ± 1.0
	IMPROVE	0.95 (0.51−1.7)	2.6 (2.3−2.8)	0.5 ± 0.3
Se	STN	1.8 (1.1−4.4)	3.5 (2.9−5.0)	2.2 ± 0.6
	IMPROVE	1.5 (1.1−2.1)	2.1 (2.0−2.5)	0.4 ± 0.2
Pb	STN	3.5 (1.8−8.1)	6.5 (6.3−7.0)	4.3 ± 2.3
	IMPROVE	3.1 (2.6−4.2)	5.1 (4.8−6.0)	0.7 ± 0.2

obstruct detection at levels well above a target element's L_c. Collocated data offer additional information near L_D, because an element that is measured below L_c on one filter may be measured above L_c on the collocated filter. L_D can then be estimated by looking at the percent of time that the element is measured above L_c on both filters as a function of the mean concentration measured on both filters. This approach to estimating L_D incorporates uncertainties associated with sample collection and preparation techniques, sample media, sensitivity of the instrument, and analytical interferences.

The collocated data come from independent measurements by equivalent methods of the same air parcel. The expected value L and the measurement distribution $\Pr(\hat{L}|L)$ can thus be assumed to be the same for both measurements. The probability that both measurements independently yield values above L_c is then the square of the probability that a

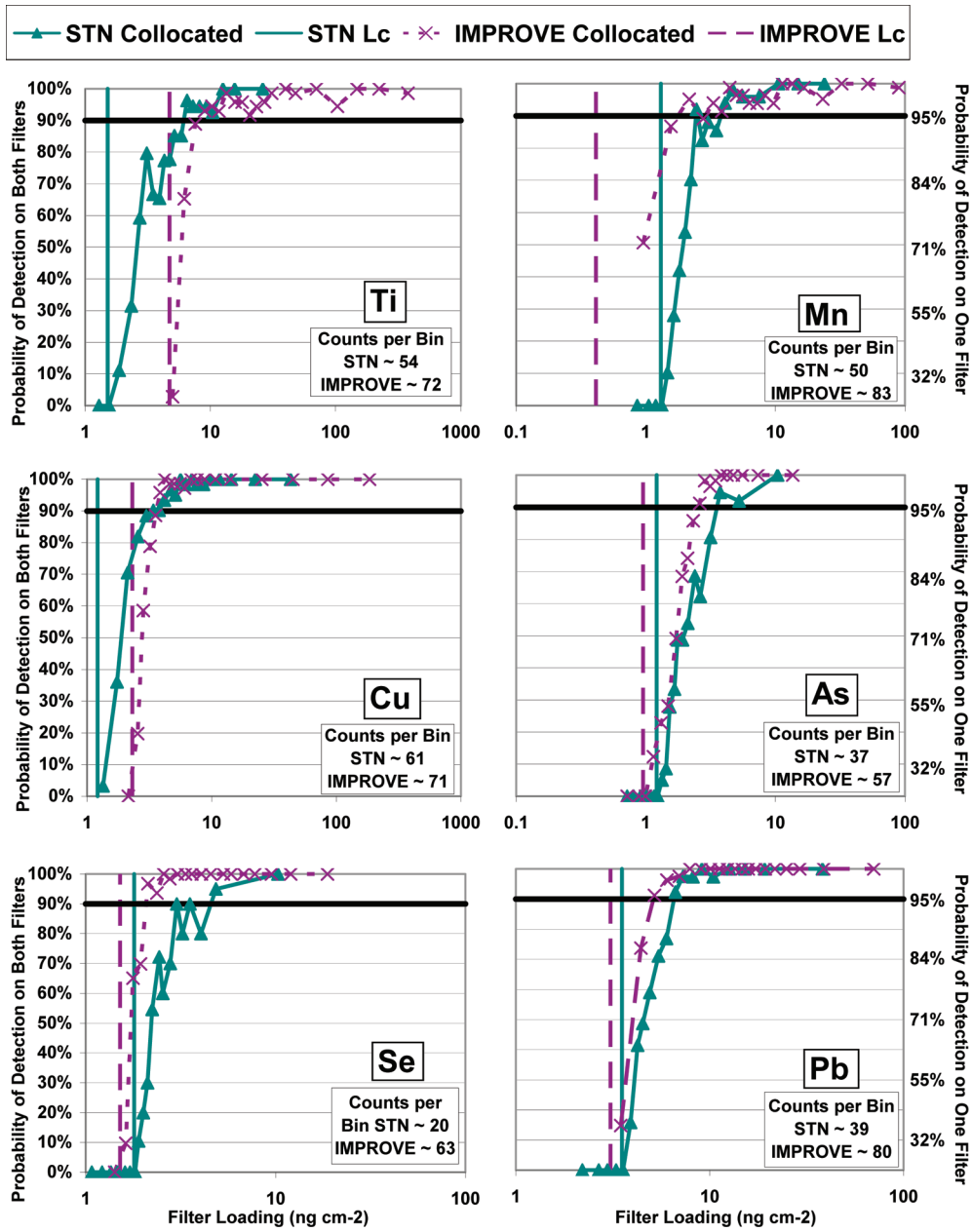

FIGURE 4. Probability of detecting the element at a loading greater than L_c in collocated filter pairs as a function of the mean reported filter loading. The L_D is set equal to the loading with a 90% probability of detecting the element above L_c on both filters which translates into a 95% probability of detecting the element above L_c on one filter.

single measurement does, $\Pr(\hat{L}_1 \geq L_c, \hat{L}_2 \geq L_c|L) = \Pr(\hat{L} \geq L_c|L)^2$. L_D can therefore be estimated as the minimum value satisfying the inequality, $\Pr(\hat{L}_1 \geq L_c, \hat{L}_2 \geq L_c|L = L_D) \geq (1 - \beta)^2$. This is the loading, estimated by the average of the reported loadings, at which both measurements report the analyte at or above L_c in at least $(1 - \beta)^2$ of the sample pairs. For $\beta = 5\%$, $(1 - \beta)^2 \cong 90\%$ is a convenient approximation.

Figure 4 shows the probability of detecting the element above L_c as a function of the mean element loading for Ti, Mn, Cu, As, Se, and Pb. The left axes show the probability of detecting the element above L_c on both filters, and the right axes show the probability of detecting the element above L_c on one filter, which is the square root of the left axis. The mean loading on the collocated filter pair is used for the x-axis. The data are grouped into equal bins according to the mean loading percentiles; each of the 20 points on the graph represents one of these bins. The counts of filter pairs included in each bin are listed in the text box in the bottom right corner of the graphs. The vertical lines indicate the L_c estimates.

The STN and IMPROVE curves shown in Figure 4 are generally similar. In some cases the curves are slightly shifted between the two networks as a result of different L_c values. The smoothness of the curve tends to improve with more data. Despite the fact that STN had more collocated data available for this analysis, IMPROVE has more collocated data above the L_c values ("counts per bin") for all the elements shown in Figure 4; this is related to the sample volume and will be addressed in more detail in the next section.

Table 1 lists L_D's estimated from the graphs in Figure 4 for a 5% type II error rate. The range in parentheses indicates the 85% to 95% probabilities of detecting the element at a loading greater than L_c on both filters, which correspond to 92% to 97% probabilities of detecting the element on one filter and 8% to 3% type II error rates.

Discusssion

Collocated data offer an opportunity to empirically estimate the limit of detection, L_D. This approach integrates the

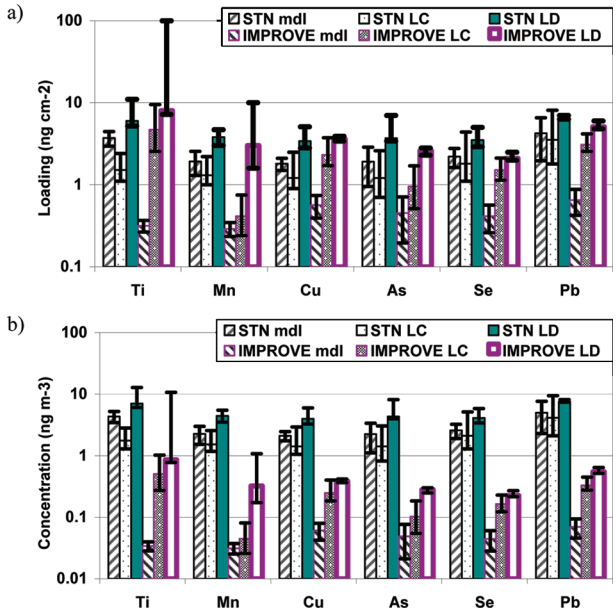

FIGURE 5. Summary of STN and IMPROVE detection limits (a) in terms of analytical measurement units (ng cm^{-2}) and (b) in terms of airborne concentrations (ng m^{-3}): reported MDL values, L_c estimates based on 95th percentile blank, and L_D estimates based on collocated data.

uncertainties from several aspects of the measurement process and thus provides the most realistic estimates of L_D. This approach can only be used for species that are measured over a range of concentrations spanning both L_c and L_D at the collocated sites.

The L_c and L_D estimates can be compared to the MDLs reported by each network. Table 1 and Figure 5a summarize the detection limits in both networks in terms of analytical measurement units, including the reported MDLs. The L_D estimates for STN and IMPROVE are very similar, suggesting that the two networks' analytical techniques are of comparable sensitivity. The idealized MDLs reported by IMPROVE are consistently lower than the empirical L_c and L_D estimates, often by an order of magnitude. The more realistic MDLs reported by STN consistently fall between the L_c and L_D estimates.

The detection limits for airborne concentrations are influenced by sample volume and sample deposit area in addition to the analytical factors considered up to this point. Our discussion has been in terms of analytical measurement units, but the data are reported and utilized in terms of airborne concentration units. Therefore, Figure 5b summarizes the detection limits in terms of airborne concentrations based on the flowrate and sample deposit areas used in the respective networks. IMPROVE uses higher flow rates and smaller deposit areas, which result in more concentrated samples by a factor of 10.9 (ratio of IMPROVE filter area per volume to STN filter area per volume). Consequently, the IMPROVE detection limits are all better than the STN detection limits in terms of ambient concentration. The lower flow rate and larger sample deposit area in STN are necessary given that most of the samplers are located in urban areas which typically experience higher $PM_{2.5}$ concentrations than IMPROVE sites. At high ambient concentrations, the IMPROVE filters are prone to clogging problems and the IMPROVE sampling configuration is thus less suitable for the STN network.

As more collocated data are obtained, the quality of these L_D estimates will improve. Also, additional collocated data from the new vacuum Cu-XRF system will allow L_D's to be estimated for the lower atomic weight elements.

Acknowledgments

This work was supported by the United States National Park Service Contract C2350-04-0050. The authors thank three anonymous reviewers and Hari Iyer for their astute observations and helpful comments and Virginia Ambrose of the USEPA for extracting STN data from AQS.

Literature Cited

(1) Currie, L. A. Nomenclature in evaluation of analytical methods including detection and quantification capabilities: (IUPAC Recommendations 1995). *Pure Appl. Chem.* **1995**, *67* (10), 1699–1723.
(2) Code of Federal Regulations (CFR), 1986. Definitions and Procedure for the Determination of the Method Detection Limit-Revision 1.11. Title 40, Part 136, Appendix B. http://ecfr.gpoaccess.gov (accessed June 20, 2007).
(3) Currie, L. A. *Detection in Analytical Chemistry: Importance, Theory, and Practice*; American Chemical Society: Washington, DC, 1988.
(4) Currie, L. A. Limits for qualitative detection and quantitative determination. *Anal. Chem.* **1968**, *40* (3), 586–593.
(5) Currie, L. A. Detection and quantification limits: origins and historical overview. *Anal. Chim. Acta* **1999**, *391*, 127–134.
(6) Currie, L. A. Detection and Quantification Capabilities and the Evaluation of Low-Level Data: Some International Perspectives and Continuing Challenges. *J. Radioanal. Nuclear Chem.* **2000**, *245* (1), 145–156.
(7) Rucker, T. L. Methodologies for the practical determination and use of method detection limits. *J. Radioanal. Nuclear Chem.* **1995**, *192* (2), 345–350.
(8) Ripp, J. Analytical Detection Limit Guidance. Wisconsin Department of Natural Resources. 1996. PUBL-TS-056-96. http://www.dnr.state.wi.us/org/es/science/lc/OUTREACH/-Publications/LOD%20Guidance%20Document.pdf (accessed July 19, 2007).
(9) Glaser, J. A.; Foerst, D. L.; McKee, G. D.; Quave, S. A.; Budde, W. L. Trace analyses for wastewaters. *Environ. Sci. Technol.* **1981**, *15* (12), 1426–1435.
(10) Hubaux, A.; Vos, G. Decision and detection limits for calibration curves. *Anal. Chem.* **1970**, *42* (8), 849–855.
(11) Jenkins, R. *X-ray Fluorescence Spectrometry*, 2nd ed.; Wiley-Interscience Publications: New York, 1999.
(12) Research Triangle Institute. Volume I Quality Assurance Project Plan Chemical Speciation of PM2.5 Filter Samples, 2005. http://www.epa.gov/ttn/amtic/files/ambient/pm25/spec/rtiqapp05.pdf (accessed May 2, 2007).
(13) University of California at Davis. Interagency Monitoring of Protected Visual Environments Quality Assurance Project Plan, 2002. http://vista.cira.colostate.edu/improve/Publications/QA_QC/IMPROVE_QAPP_R0.pdf (accessed July 20, 2007).
(14) University of California at Davis. Data report for elemental analysis of IMPROVE samples collected during January, February and March 2005, 2006. http://vista.cira.colostate.edu/improve/Data/QA_QC/QAQC_UCD.htm (accessed August 8, 2007).
(15) White, W. H. Changes in sodium data quality, 2007. http://vista.cira.colostate.edu/improve/Data/QA_QC/Advisory/da0017/da0017_Na.pdf (accessed June 29, 2007).
(16) Harrison, J. F.; Eldred, R. A. Automatic data acquisition and reduction for elemental analysis of aerosol samples. *Adv. X-Ray Anal.* **1974**, *17*, 560–583.
(17) Research Triangle Institute. Standard Operating Procedure for the X-Ray Fluorescence Analysis of PM2.5 Deposits on Teflon Filters, 2004. http://www.epa.gov/ttnamti1/files/ambient/pm25/spec/xrfsop.pdf(accessed August 20, 2007).
(18) Research Triangle Institute. Annual Data Summary Report for the Chemical Speciation of PM 2.5 Filter Samples Project, 2007. http://www.epa.gov/ttn/amtic/files/ambient/pm25/spec/RTI_0885800−05%20Data%20Sum%20Rpt.pdf (accessed September 20, 2007).
(19) Hyslop, N. P.; White, W. H. An evaluation of interagency monitoring of protected visual environments (IMPROVE) collocated precision and uncertainty estimates. Atmos. Environ., in press. http://dx.doi.org/10.1016/j.atmosenv.2007. 06.053.
(20) Flanagan, J. B.; Jayanty, R K. M.; Peterson, M. R. PM2.5 Speciation Trends Network: Evaluation of Whole-System Uncertainties Using Data from Sites with Collocated Samplers. *Air Waste Manage. Assoc.* **2006**, *56*, 492–499.

ES7025196